

Preparation and High-Frequency Dielectric Properties of Polytetrafluoroethylene Reinforced Bismaleimide-Triazine Resin Glass Fiber Composites

Suchat Delgado¹, Nacarid Bravo¹, Jorge Raita^{2,*}

¹ The Joint Graduate School for Energy and Environment (JGSEE), King Mongkut's University of Technology Thonburi, Prachauthit Road, Bangmod, Bangkok 10140, Thailand

² Area de Bioproductos, Unidad de Desarrollo Tecnológico (UDT), Universidad de Concepción (UdeC), Av. Cordillera 2634, Parque Industrial Coronel, Coronel, Biobío, Chile

*Corresponding author: JorgeRaita@udt.cl

Abstract. Addressing the stringent requirements of 5G/6G high-frequency and high-speed communication technologies for printed circuit board (PCB) substrates, this study designed and prepared a polytetrafluoroethylene (PTFE)-filled modified bismaleimide-triazine (BT) resin/glass fiber (GF) composite. The glass fiber cloth was surface-modified with silane coupling agent KH570 to enhance interfacial bonding, and low-dielectric PTFE filler was introduced into the pores of the glass fiber cloth via a high-temperature and high-pressure lamination process; the influence mechanism of PTFE content on the comprehensive properties of the composite was systematically investigated. Results indicate that when the PTFE mass fraction is 5%, the composite achieves optimal comprehensive performance: the dielectric constant (Dk) and dielectric loss (Df) are 4.3 and 0.006 at 1 MHz, and 3.4 and 0.003 at 10 GHz, respectively; the glass transition temperature (T_g) increases to 250°C (approximately 25°C higher than that of the pure BT system), the char yield at 800°C reaches 76.63% (an increase of about 17.55%), the flexural strength remains at 574.7 MPa, and the water contact angle increases to 86.5°. Mechanism analysis reveals that the introduction of PTFE significantly improves the high-frequency dielectric properties of the composite by reducing the polarization degree, filling pores to decrease interfacial polarization losses, and restricting the orientation movement of polar groups. Simultaneously, the high bond energy of C-F bonds endows the composite with enhanced thermal stability. However, the high coefficient of thermal expansion (CTE) of PTFE raises the CTE of the composite to approximately $45 \times 10^{-6} \text{ } ^\circ\text{C}^{-1}$, which requires further optimization. This material system achieves a significant improvement in dielectric properties while maintaining the high heat resistance and good processability of BT resin, providing a cost-competitive substrate solution for mid-to-high frequency applications such as 5G millimeter-wave antennas and radio frequency front ends.

Keywords: composite; BT resin; PTFE; dielectric properties; coefficient of thermal expansion; 5G/6G communication

Received on 15 Jan 2026, Accepted on 15 April 2026, Published on 15 May 2026

Copyright © 2026 Suchat Delgado *et al.* licensed to JGEEE. This is an open access article distributed under the terms of the CC BY-NC-SA 4.0, which permits copying, redistributing, remixing, transformation, and building upon the material in any medium so long as the original work is properly cited.

1 Introduction

In recent years, with the large-scale commercialization of 5G communication technology and the accelerated research and development of 6G technology, electronic products and printed circuit boards (PCBs) have continuously evolved toward high frequency, high speed, miniaturization, and integration [1-3]. The 5G communication system is primarily deployed in two major frequency bands: Sub-6GHz (3.5–7.125 GHz) and millimeter wave (24–52 GHz), while 6G technology is expected to expand further into the terahertz band (100 GHz–1 THz). During the transmission of high-frequency signals, signal integrity faces severe challenges: firstly, signal attenuation caused by dielectric loss; secondly, signal reflection and delay caused by mismatched dielectric constants; and thirdly, layer misalignment caused by insufficient dimensional stability of the material. According to transmission line theory, signal attenuation is proportional to the dielectric loss factor (Df). In the millimeter-wave band, even minute dielectric losses can lead to significant signal attenuation, severely affecting communication quality.

For different application scenarios, the performance requirements of PCB substrates vary. In 5G millimeter-wave antenna modules, Copper Clad Laminates (CCLs) are required to have stable dielectric constants ($D_k < 3.5$, $D_f \leq 0.005$) within the 24–52 GHz band to ensure antenna radiation efficiency and beam pointing accuracy. On one hand, in radio frequency front-end modules, components such as power amplifiers generate substantial heat during operation, with local temperatures often exceeding 200°C. If the glass transition temperature (T_g) of the substrate is too low, softening and deformation will occur at high temperatures, leading to circuit impedance drift, signal distortion, or even module failure. Furthermore, in multilayer High Density Interconnect (HDI) antenna substrates, where high-frequency signal wiring density is high and layer counts are numerous (often exceeding 10 layers), multiple high-temperature pressing and soldering thermal shocks during processing demand excellent thermal dimensional stability from the substrate, making high T_g a key indicator for ensuring long-term reliability. On the other hand, PCB multilayering is an inevitable trend for increasing integration; however, mismatches in the coefficient of thermal expansion (CTE) between material layers induce cumulative thermal stress during thermal cycling, leading to reliability issues such as plated through-hole (PTH) cracking and delamination. Especially in high-frequency applications like millimeter-wave antennas, where microstrip line widths and spacings have reached the micron level, slight material expansion can cause impedance mutations and signal reflection, severely affecting antenna efficiency and beam pointing accuracy. Therefore, a low CTE (especially in the Z-axis direction) is a core indicator for ensuring signal integrity and structural reliability in high-frequency circuits.

As the core substrate of PCBs, the performance of CCLs depends largely on the adopted resin system. Currently, commonly used resin systems include epoxy resin, cyanate ester resin, bismaleimide resin, polyphenylene ether resin, and hydrocarbon resin [1-3]. Epoxy resin dominates the market due to its excellent processability and cost advantages, yet its dielectric properties struggle to meet the demands of high-frequency applications [4]; although Polyphenylene Oxide (PPO) and hydrocarbon resins possess excellent dielectric properties ($D_k \approx 2.4-2.6$, $D_f \approx 0.001-0.002$), their T_g is relatively low ($< 200^\circ\text{C}$), and their CTE is relatively high, facing reliability challenges in high-temperature, high-integration scenarios [5]. Although companies like NVIDIA utilize hydrocarbon resins as substrates in certain high-performance computing cards, their applicable scenarios are typically modules with optimized heat dissipation conditions and relatively fewer layers; for fields requiring high heat resistance and high dimensional stability, such as millimeter-wave antennas and high-layer count server backplanes, there is still a lack of substrate solutions with balanced comprehensive performance. Consequently, developing novel resin systems that combine low dielectric properties, high heat resistance, and excellent dimensional stability has become an urgent industry requirement.

Bismaleimide-triazine (BT) resin, copolymerized from bismaleimide (BMI) and cyanate ester (CE), combines the high T_g and heat resistance of BMI with the excellent dielectric properties and low shrinkage rate of CE, and is considered a highly promising matrix material for high-frequency and high-speed CCLs. Wang Xu et al. [6] prepared BT resin by copolymerizing BMI-80 resin with cyanate ester, impregnated glass fibers to prepare glass fiber-reinforced BT composites, and studied their structure and properties. Wang Qi [7] modified BMI-80 with allylated fluorinated polysulfone and cyanate ester; the prepared fiber-reinforced composite improved thermal, mechanical, and dielectric properties. However, in the aforementioned studies, the pores of the glass fiber cloth were filled solely by the resin matrix itself; if filled with materials possessing superior dielectric properties, the dielectric performance of the composite could be further enhanced.

Polytetrafluoroethylene (PTFE), owing to its highly symmetrical molecular structure (helical conformation of the $-\text{CF}_2-\text{CF}_2-$ main chain) and extremely low polarization rate of C-F bonds, possesses ultra-low dielectric constant ($D_k \approx 1.9-2.1$) and dielectric loss ($D_f < 0.0005$), earning it the title of "Plastic King" [8]. After filling with PTFE, its low-loss characteristics cover the pore regions of the glass fiber cloth, reducing additional losses caused by air/resin interfaces within the pores, decreasing the overall dielectric loss from 0.005–0.02 to below 0.001, and significantly reducing attenuation and delay of high-frequency signals. However, research by Fang Hongqiang at Northwestern Polytechnical University [9] indicates that GF-PTFE composites suffer from difficulties in processing, complex molding processes, poor adhesion, and insufficient mechanical strength, limiting their widespread application.

Based on the above analysis, this study proposes an innovative material design strategy: utilizing PTFE to fill the

pores of glass fiber cloth and employing BT resin—which possesses excellent comprehensive properties—as the matrix [10-11], to prepare PTFE/BT/GF composites via high-temperature and high-pressure molding technology. This design aims to fully leverage the ultra-low dielectric properties of PTFE and the high heat resistance and good processability of BT resin, achieving complementary advantages in performance. The study systematically investigates the influence of PTFE content on the microstructure, dielectric properties (1 MHz–12 GHz), thermal properties, mechanical properties, and water absorption properties of the composite, deeply analyzing the dielectric relaxation mechanisms, the causes of increased CTE, and potential improvement strategies, providing a theoretical basis and experimental support for the development of high-frequency and high-speed CCL substrates.

2. Experimental Section

2.1 Main Raw Materials

Bisphenol A cyanate ester (BADCy, purity 98%), Aladdin; N,N'-(4,4'-methylenediphenyl)bismaleimide (BMI, purity 98%), Aladdin; 2-methylimidazole (purity 98%), Aladdin; Polytetrafluoroethylene emulsion (PTFE, solid content 60%), DuPont; E-glass fiber cloth (GF, monofilament diameter 9 μm , aperture 0.18 mm), Jushi Group; Acetic acid (CH_3COOH , purity 36%), Sinopharm Chemical Reagent; Anhydrous ethanol ($\text{C}_2\text{H}_5\text{OH}$, purity $\geq 99.7\%$), Sinopharm Chemical Reagent; Deionized water, self-made; γ -aminopropyltriethoxysilane (KH550, purity 98%), Aladdin; γ -methacryloxypropyltrimethoxysilane (KH570, purity 98%), Aladdin; 3-chloropropyltrimethoxysilane (CTS, purity 98%), Aladdin.

2.2 Preparation of PTFE/BT/GF Composites

2.2.1 Pretreatment of Glass Fiber Cloth

Glass fiber cloth was cut into 15 cm \times 15 cm square specimens for later use. To enhance the interfacial bonding between the glass fiber cloth, PTFE, and the resin, surface treatment was performed using silane coupling agents [12]. This study compared the effects of three coupling agents: KH570, KH550, and CTS. Firstly, the silane coupling agent was mixed with ethanol and deionized water (mass ratio 9:1) to prepare a 2 wt% solution, adjusted to weak acidity ($\text{pH} \approx 4\text{--}5$) with acetic acid, and hydrolyzed at 80°C for 6 h. Subsequently, the glass fiber cloth was immersed in the hydrolyzed coupling agent solution for 3 h, removed, and dried in an oven at 100°C for 2 h.

2.2.2 Dilution and Demulsification of PTFE Dispersion

An appropriate amount of concentrated PTFE dispersion (60%) was taken, and deionized water was added to dilute it to target mass fractions (1%, 3%, 5%, 7%, 9%). The diluted PTFE emulsion was stirred at high speed (2000 r/min) for 5 h using a high-speed stirrer to achieve demulsification, resulting in a uniform PTFE emulsion.

2.2.3 Preparation of PTFE/GF Preforms

The glass fiber cloth, treated with silane coupling agent and dried, was immersed into the aforementioned PTFE emulsion, soaked for 60–120 s, and then removed; this process was repeated three times to ensure thorough impregnation. Subsequently, it was placed in an oven at 110°C for pre-drying for 30 min, removed, and cooled to room temperature for later use.

2.2.4 Preparation of BT Resin

60 g of cyanate ester and 20 g of bismaleimide were weighed into a beaker, melted at 170°C for 2 h for prepolymerization. Then, 2.4 g of 2-methylimidazole was added as a curing accelerator, stirred thoroughly and mixed evenly to obtain the BT resin prepolymer.

2.2.5 Preparation of PTFE/BT/GF Composites

The glass fiber cloth impregnated with PTFE and pre-dried was laid flat into a self-made mold, and the pre-

polymerized BT resin was poured in. The mold was placed in a vacuum oven at 120°C for 30 min to remove bubbles and allow the resin to fully impregnate the glass fiber cloth. After impregnation, a high-temperature and high-pressure stepwise curing process was adopted: gelation at 140°C and 2 MPa, followed by processing at 160°C and 5 MPa for 1 h, 180°C and 8 MPa for 2 h, 200°C and 10 MPa for 2 h, and 220°C and 10 MPa for 2 h. After curing, the pressure was maintained while naturally cooling to room temperature, and the mold was opened to obtain the PTFE/BT/GF composite sheet.

2.3 Characterization and Performance Testing

Fourier Transform Infrared Spectroscopy (FT-IR): Tested using a Shimadzu IR Prestige-21 spectrometer (Japan), scanning range 400–4000 cm⁻¹, resolution 4 cm⁻¹, used to analyze functional group changes on the surface of glass fiber cloth after silane coupling agent modification.

Scanning Electron Microscopy (SEM): Observed using a Gemini ZEISS electron microscope (Germany) to examine the surface morphology of glass fiber cloth, cross-sectional morphology of composites, and PTFE distribution, acceleration voltage 5 kV.

Thermogravimetric Analysis (TGA): Tested using a Netzsch STA449F3 thermogravimetric analyzer (Germany) under a nitrogen atmosphere (flow rate 100 mL/min), heating from 40°C to 800°C at a rate of 10 K/min, sample mass 3–5 mg.

Dynamic Mechanical Analysis (DMA): Tested using a Netzsch DMA 242E analyzer (Germany), three-point bending mode, specimen dimensions 60 mm × 10 mm, thickness ≥0.5 mm, heating rate 5°C/min, amplitude 15–20 μm, frequency 1 Hz.

Dielectric Property Testing: Low-frequency dielectric properties were tested using an Agilent E4980A precision LCR meter, frequency range 20 Hz–1 MHz; high-frequency dielectric properties were tested using a Chuangyuan Tech T5260A-2KA vector network analyzer, employing the resonant cavity method for the 8–12 GHz band, specimen size 50 mm × 50 mm.

Thermomechanical Analysis (TMA): Tested using a Netzsch TMA402F1 thermomechanical analyzer (Germany) to measure the Z-axis coefficient of thermal expansion (CTE) of composites, load 0.05 N, heating rate 10°C/min, test temperature range 50–200°C.

Mechanical Property Testing: Flexural properties were tested using a Shenzhen Sansi Zongheng UTM420HA universal testing machine, specimen dimensions 76.2 mm × 25.4 mm × 1.57 mm, span 25.4 mm, test speed 0.76 mm/min; impact properties were tested using a Chengde Jinjian XJUD-5.5 electronic cantilever impact tester.

Water Absorption Rate Testing: Tested under ambient and high-temperature conditions; specimen size 10 cm × 10 cm, weighed after drying (W₁), immersed in distilled water (ambient 23°C±2°C, 24 h; high temp 100°C±2°C, 2 h), wiped dry and weighed (W₂), calculated as (W₂ - W₁)/W₁×100%.

Water Contact Angle Testing: Tested using a Dataphysics OCA20 contact angle goniometer (Germany), analyzed using the baseline circle method for water droplets on the material surface.

3. Results and Discussion

3.1 Chemical Structure of Silane Coupling Agent Modified Glass Fiber Cloth

Figure 1 shows the infrared spectra of glass fiber cloth modified with different silane coupling agents. The sample treated with KH570 exhibited strong absorption peaks near 801 cm⁻¹ and 1028 cm⁻¹, corresponding to the symmetric and asymmetric stretching vibrations of Si–O–Si bonds, respectively, indicating that the coupling agent

formed a cross-linked network structure on the glass fiber surface. Absorption peaks appearing at 2955 cm^{-1} and 2838 cm^{-1} correspond to the symmetric stretching vibrations of $-\text{CH}_3$ and $-\text{CH}_2$, respectively, suggesting that the methacryloxypropyl group of KH570 was successfully grafted onto the glass fiber surface. In contrast, samples treated with KH550 and CTS did not show obvious C–H stretching vibration peaks, indicating that KH570 had a higher grafting efficiency. Furthermore, the C=C double bonds in KH570 can undergo copolymerization with allyl radicals generated during the curing process of BT resin, forming chemical bonding and further enhancing interfacial bonding strength [13].

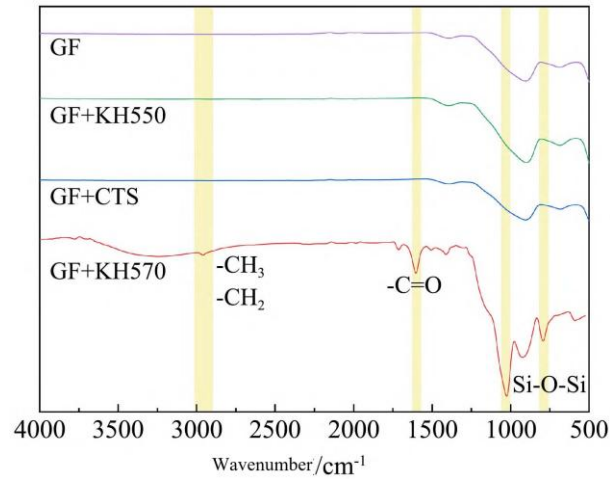


Figure 1 FT-IR spectra of glass fiber cloth modified with different silane coupling agents

3.2 Microstructure Morphology of Composites

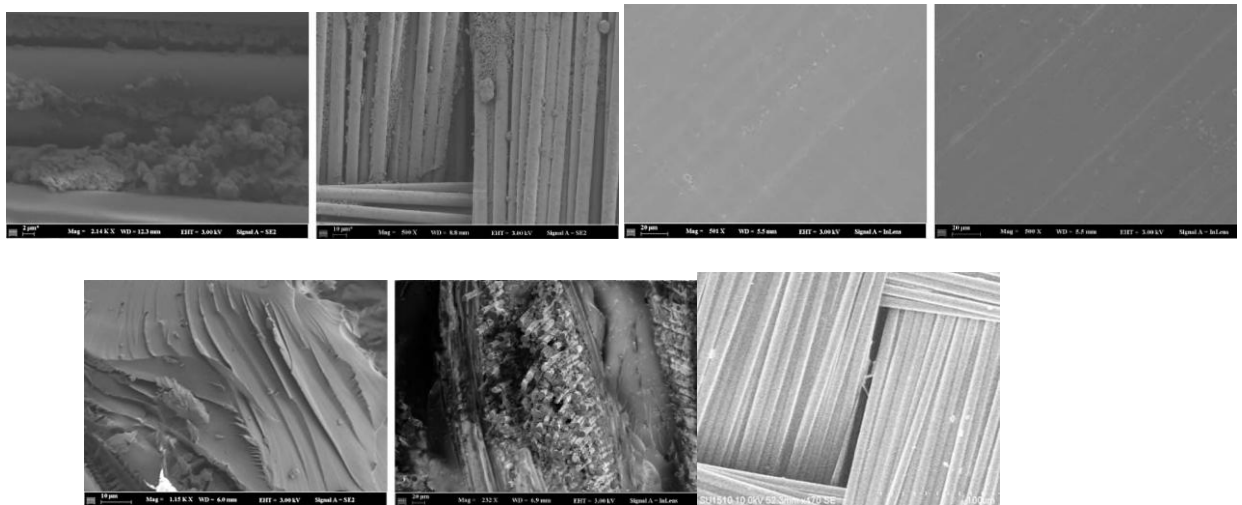


Figure 2 SEM images of composites with different PTFE contents

Figure 2 shows SEM images of composites with different PTFE contents. Figure 2(a) shows that compared to the original warp-weft woven structure of the glass fiber (Figure 2(g)), when the PTFE mass fraction was 5%, PTFE uniformly filled the pores of the glass fiber cloth without significant agglomeration; fibers and the resin matrix were tightly bound, with no obvious voids at the interface. This benefits from KH570 improving the wettability between fibers and resin, and the good dispersibility of the PTFE emulsion ensuring uniform distribution of filler within the pores. Figure 2(b) shows that when the PTFE mass fraction increased to 9%, obvious agglomeration phenomena were observed, with agglomerate sizes reaching 5–10 μm , and interface debonding occurred in some areas. This is because excess PTFE exceeded the pore capacity of the glass fiber cloth, and surplus PTFE agglomerated within the resin matrix. Figures 2(c) and 2(d) display smooth and dense surfaces for both 5% and

9% PTFE composites, with no visible defects. Figures 2(e) and 2(f) show the cross-sectional morphologies of 5% and 9% PTFE composites, respectively; the 5% sample exhibits a smooth fracture surface with good fiber-matrix bonding, whereas the 9% sample shows a rough fracture surface with obvious fiber pull-out and matrix cracking, indicating that excess PTFE impairs interfacial bonding strength.

3.3 Dielectric Properties of Composites

3.3.1 Low-Frequency Dielectric Properties

Figure 3 illustrates the variation of low-frequency dielectric properties of composites with PTFE content at 1 kHz–1 MHz. Figure 3(a) shows that the dielectric constant of the BT/GF composite without PTFE was approximately 4.8 at 1 MHz, with a dielectric loss of about 0.01. With the introduction of PTFE, both the dielectric constant and dielectric loss of the composite showed a trend of decreasing first and then slightly rebounding. When the PTFE mass fraction was 5%, the dielectric constant dropped to 4.3, a reduction of about 12.2% compared to the pure BT system; the dielectric loss dropped to 0.006, a reduction of about 40%.

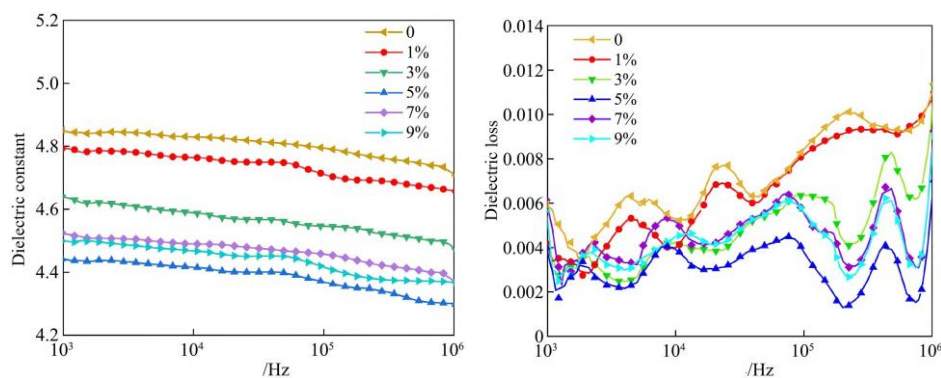


Figure 3 Low-frequency dielectric properties of composites

The improvement in dielectric properties is mainly attributed to the following factors: (1) PTFE itself possesses an extremely low dielectric constant ($D_k \approx 1.9$) and dielectric loss ($D_f \approx 0.0002$), and its introduction lowers the overall polarization degree of the composite [14]; (2) PTFE fills the pores of the glass fiber cloth, reducing charge accumulation at the interface between air ($D_k \approx 1.0$) in the pores and the resin matrix ($D_k \approx 4.5-5.0$), thereby decreasing interfacial polarization loss [15]; (3) Silane coupling agent modification enhances the interfacial bonding between glass fiber and resin, restricting molecular chain motion at the interface and reducing orientation polarization loss.

Figure 3(b), the dielectric loss frequency spectrum, shows that the composite without PTFE exhibits three distinct relaxation peaks within the test frequency band. The relaxation peak around 7 kHz is attributed to Maxwell-Wagner interfacial polarization at the glass fiber/resin interface. When two materials with different dielectric constants and conductivities are composited, charge accumulation occurs at the interface under an external electric field, forming macroscopic dipole moments, manifesting as relaxation loss peaks at specific frequencies. The relaxation peak around 23 kHz corresponds to dipolar orientation polarization arising from the interaction of polar groups (such as Si-OH) introduced by surface modification of glass fibers and polar groups (triazine rings, imide rings) in the BT resin molecular chains. The relaxation peak around 225 kHz corresponds to side-chain relaxation (β -relaxation) of restricted molecular chains in the BT resin.

After adding PTFE, all three relaxation peaks exhibited varying degrees of shift and intensity change. This is primarily because the PTFE molecular chain is highly symmetrical and extremely rigid; the main chain consists of C-C single bonds, and the side chains are perfluorinated groups, meaning molecular chain motion requires overcoming high energy barriers, resulting in significantly longer relaxation times for PTFE compared to kinetic units like triazine rings and imide rings in BT resin. When PTFE is blended with BT resin, the difference in molecular chain dynamics leads to the formation of a continuous relaxation time distribution, causing the original relaxation peaks to shift towards lower frequencies and broaden. Additionally, the introduction of PTFE may generate new PTFE/BT interfacial relaxation peaks, superimposing with original peaks to cause peak shifting and

broadening.

3.3.2 High-Frequency Dielectric Properties

Figure 4 shows the dielectric properties of composites in the 8–12 GHz band (X-band). Figure 4(a) indicates that the dielectric constant of the composite without PTFE was approximately 3.7 (10 GHz); with increasing PTFE content, the dielectric constant showed a monotonic decreasing trend. When the PTFE mass fraction was 5%, the dielectric constant dropped to 3.4 (10 GHz), a reduction of about 8.1% compared to the pure BT system. The decrease in dielectric constant stems from the low polarizability of PTFE: the electron polarization rate and dipole moment of the C–F bond are extremely low, and the strong electronegativity of fluorine atoms effectively fixes the electron cloud, inhibiting electronic polarization; simultaneously, the high bond energy and rigidity of the C–F bond limit chain segment motion under high-frequency alternating electric fields, further weakening orientation polarization.

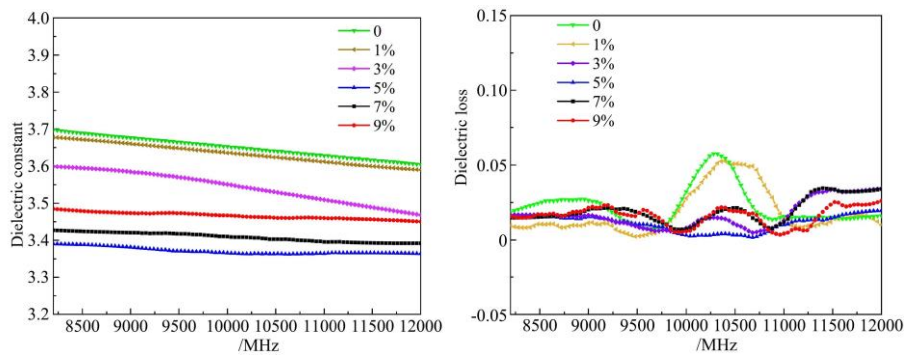


Figure 4 High-frequency dielectric properties of composite materials

Figure 4(b) shows that the dielectric loss of the composite decreases initially and then increases with PTFE content, reaching a minimum value of 0.003 (10 GHz) at 5% PTFE, a reduction of about 50% compared to the pure BT system. The reduction in dielectric loss benefits from the filling of pores by PTFE, which reduces charge accumulation and interfacial polarization loss at air/resin interfaces within the glass fiber cloth pores. It is worth noting that the composite without PTFE exhibits a distinct relaxation peak near 10 GHz, mainly attributed to the dipolar relaxation of polar groups (imide groups, cyanate groups) in the BT resin. When the dipolar relaxation frequency matches the test frequency (10 GHz), dipoles cannot rapidly orient with the alternating electric field, overcoming internal friction to generate significant energy loss, forming a loss peak. After adding PTFE, this relaxation peak gradually disappears, mainly due to: (1) PTFE molecular chains intertwining between BT resin chains restrict the rotational freedom of polar groups, reducing the orientation mobility of dipoles; (2) The low polarity of PTFE dilutes the concentration of polar groups in the system, greatly attenuating dipolar relaxation intensity; (3) Improved interfacial bonding after PTFE fills pores reduces additional losses caused by interfacial defects. However, when the PTFE mass fraction exceeds 5%, dielectric loss rebounds slightly, which is associated with increased interfacial defects due to excess PTFE agglomeration.

Table 1 Comparison of dielectric properties of different high-frequency CCL substrates (10 GHz)

Material Type	Dk	Df	Tg(°C)
FR-4 Epoxy Resin	4.3–4.8	0.015–0.020	130–180
Hydrocarbon Resin	2.6–3.0	0.002–0.004	>250
LCP	≈2.5	≈0.002	≈280
PTFE	≈2.1	≈0.0005	≈327
This study (5% PTFE/BT/GF)	3.4	0.003	250

Table 1 lists the dielectric properties of the PTFE/BT/GF composite prepared in this study compared with commercial high-frequency CCL substrates. Table 1 shows that the dielectric properties (Dk=3.4, Df=0.003, 10 GHz) of the 5% PTFE modified BT/GF composite are superior to traditional FR-4 epoxy resin (Dk≈4.5, Df≈0.015), close to commercial hydrocarbon resins (Dk ≈2.6–3.0, Df≈0.002–0.004), but still lag behind LCP (Dk≈2.5, Df

≈0.002) and PTFE substrates ($D_k \approx 2.1$, $D_f \approx 0.0005$). This is mainly because the polarity of BT resin itself is higher than that of hydrocarbon resins and PTFE, and the introduction of glass fiber ($D_k \approx 6.1$) increases the overall dielectric constant. Nevertheless, this material holds advantages in cost, processability, and heat resistance, making it suitable for mid-to-high frequency application scenarios sensitive to cost but requiring certain dielectric performance.

3.4 Thermal Properties of Composites

3.4.1 Glass Transition Temperature and Storage Modulus

Figure 5 shows the DMA curves of the composites. Figure 5(a), the loss factor ($\tan \delta$) curve, indicates that the glass transition temperature (T_g) of the pure BT resin composite is approximately 225°C. With the addition of PTFE, T_g gradually increases; when the PTFE mass fraction is 5%, T_g reaches 250°C, an increase of about 25°C compared to the pure BT system. The elevation of T_g may be attributed to the following mechanisms: (1) The crystallinity of PTFE induces regular arrangement of BT resin molecular chains, increasing local crystallinity and intermolecular forces [16]; (2) PTFE molecular chains are highly rigid; their introduction restricts BT resin segment motion, forming physical cross-linking points; (3) Glass fibers act as heterogeneous nucleation sites for PTFE crystallization, lowering the nucleation energy required for PTFE crystallization.

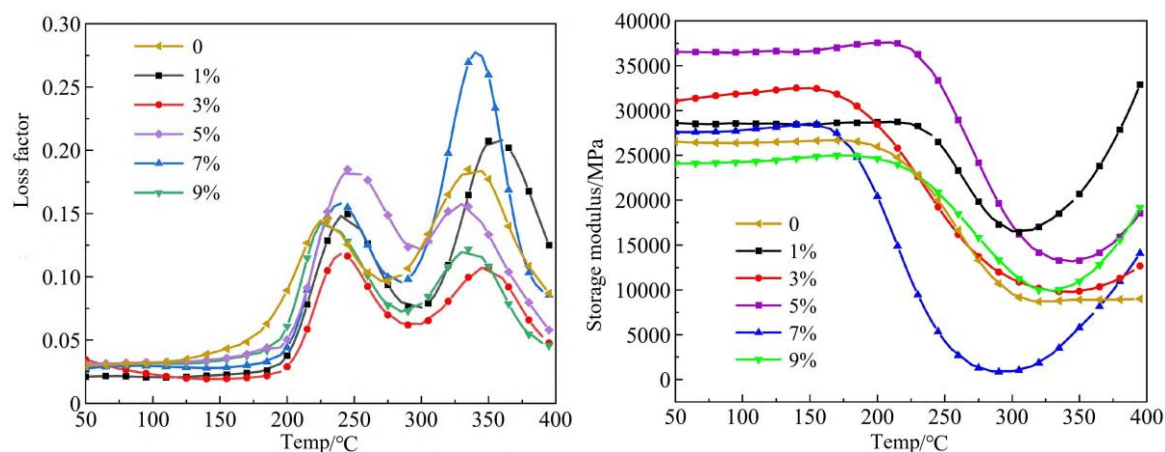


Figure 5 DMA curves of composites

Figure 5(b), the storage modulus curve, shows that the storage modulus of the composite initially increases and then decreases with increasing PTFE content, reaching a maximum value of 36000 MPa (30°C) at 5%, an increase of about 10000 MPa compared to the pure BT system. The increase in storage modulus indicates enhanced material rigidity, related to the high modulus characteristics of PTFE and its restrictive effect on resin matrix segment motion [17]. Notably, the storage modulus shows an upward trend after 300°C, mainly due to PTFE crystallization. Under the combined effect of pressure and temperature, the diffusion and rearrangement of PTFE molecular chains are optimized, and increased crystallinity leads to a rebound in storage modulus. The peak around 340–350°C corresponds to the glass transition of the triazine ring formed by the self-polymerization of cyanate monomers.

3.4.2 Thermal Stability

Figure 6 shows the TGA and DTG curves of composites under N_2 atmosphere, with thermal property data listed in Table 2. Figure 6(a) TGA curve shows that all samples exhibit good thermal stability, with char yields at 800°C exceeding 55%. When the PTFE mass fraction was 5%, the composite's T_{d5} and T_{d10} reached 319.9°C and 391.9°C, respectively, and the char yield at 800°C was as high as 76.63%, an increase of about 17.55% compared to the sample without PTFE (59.08%).

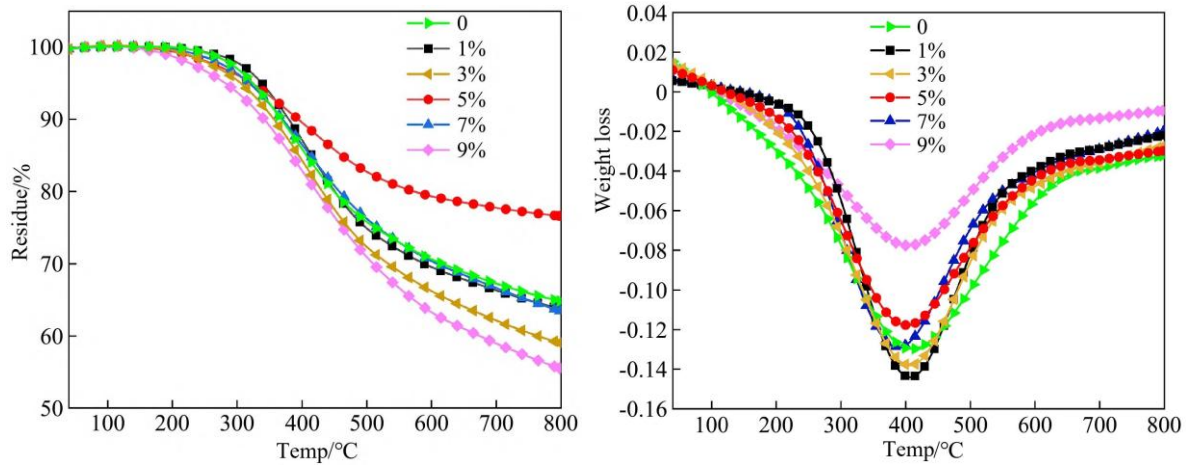


Figure 6 Thermogravimetric analysis of composites

The improvement in thermal stability is mainly attributed to the high bond energy (≈ 485 kJ/mol) of the C–F bond in the PTFE molecular chain and the tight wrapping protection of the carbon chain by fluorine atoms, effectively inhibiting the fracture and thermal decomposition of BT resin molecular chains at high temperatures [18]. However, excessively high PTFE content (e.g., 9%) leads to stress concentration due to interfacial defects and agglomeration, instead causing a decline in thermal stability, with Td5 dropping to 280.8°C . Figure 6(b) DTG curve shows that the maximum decomposition rate temperature (Tmax) of the 5% PTFE sample shifts towards higher temperatures by about 15°C , further confirming the beneficial effect of PTFE on material thermal stability.

Table 2 Thermal properties of composites with different PTFE contents

PTFE Mass Fraction (%)	Td5($^{\circ}\text{C}$)	Td10($^{\circ}\text{C}$)	Char Yield at 800 $^{\circ}\text{C}$ (%)
0	304.6	355.6	59.08
1	324.4	367.4	64.85
3	338.1	379.0	63.82
5	319.9	391.9	76.63
7	318.9	366.4	63.49
9	280.8	339.8	55.51

3.4.3 Coefficient of Thermal Expansion (CTE)

Figure 7 shows the coefficient of thermal expansion (CTE) of composites within the range of $50\text{--}200^{\circ}\text{C}$. Figure 7 indicates that with increasing PTFE content, the CTE of the composite shows a clear upward trend. The CTE of the pure BT/GF composite is approximately $32 \times 10^{-6} \text{ }^{\circ}\text{C}^{-1}$ (Z-axis direction); when the PTFE mass fraction is 5%, the composite's CTE rises to about $45 \times 10^{-6} \text{ }^{\circ}\text{C}^{-1}$, an increase of about 40%; when the PTFE mass fraction increases to 9%, the composite's CTE further rises to about $58 \times 10^{-6} \text{ }^{\circ}\text{C}^{-1}$.

The reasons for the increase in CTE can be analyzed from the following aspects: (1) PTFE itself has an extremely high coefficient of thermal expansion ($100\text{--}130 \times 10^{-6} \text{ }^{\circ}\text{C}^{-1}$, $25\text{--}100^{\circ}\text{C}$), far higher than BT resin ($35\text{--}45 \times 10^{-6} \text{ }^{\circ}\text{C}^{-1}$) and glass fiber ($5.5 \times 10^{-6} \text{ }^{\circ}\text{C}^{-1}$). During heating, PTFE molecular chains have high degrees of freedom of motion and easily acquire more thermal energy, leading to an increase in CTE [19]. (2) CTE mismatch between the matrix and filler leads to accumulation of thermal stress; during thermal cycling, high expansion of PTFE generates shear stress at the interface, and when the stress exceeds the interfacial bonding strength, microcracks and debonding occur, further increasing the overall CTE [20]. (3) Excessive PTFE agglomeration forms interfacial defects that

provide extra free space for thermal expansion, exacerbating the rise in CTE.

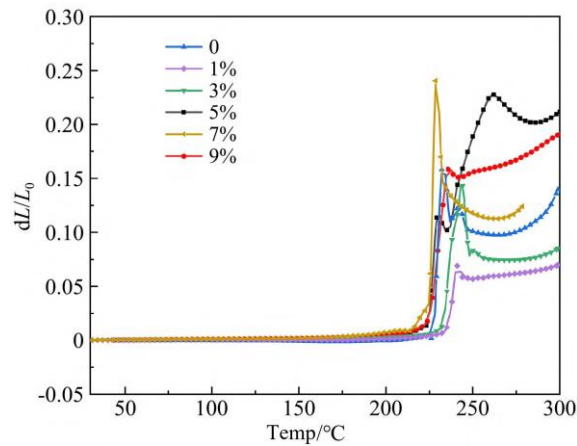


Figure 7 Coefficient of thermal expansion of composites

The impact of increased CTE on PCB applications cannot be ignored. During the manufacturing process of PCB multilayer boards, Z-axis CTE mismatch can lead to stress concentration in plated through-holes (PTH), causing PTH cracking or copper foil breakage failures during thermal shock (such as soldering processes). According to IPC-4101 standards, the Z-axis CTE of high-frequency CCLs should be controlled below $60 \times 10^{-6} \text{ } ^\circ\text{C}^{-1}$. The CTE of the 5% PTFE sample in this study ($45 \times 10^{-6} \text{ } ^\circ\text{C}^{-1}$) meets this requirement but still leaves room for further optimization.

3.5 Mechanical Properties of Composites

Figure 8 shows the flexural strength and impact strength of the composites. Figure 8 indicates that the flexural strength of the composite without PTFE was 589.5 MPa. When the PTFE mass fraction was below 5%, the flexural strength of the composite remained stable; specifically, the flexural strength of the 5% PTFE composite was 574.7 MPa, a decrease of only 2.5% compared to the pure BT system. This benefits from KH570 improving interfacial bonding, and PTFE forming good mechanical interlocking with the resin matrix after filling pores, effectively transferring external stress. However, when the PTFE mass fraction increased to 9%, the flexural strength of the composite dropped to 525 MPa, a decrease of about 11%, yet it still meets industrial application requirements.

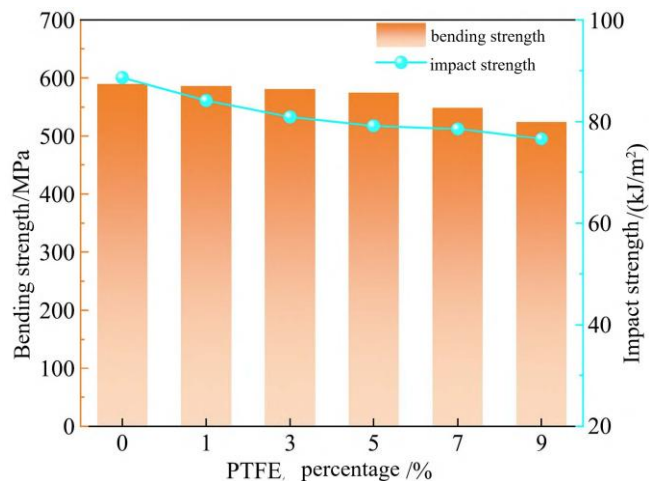


Figure 8 Mechanical properties of composites

Figure 8 also shows that the impact strength of the composite decreased slightly with the addition of PTFE; the impact strength of the composite without PTFE was 88.6 kJ/m^2 , that of the 5% PTFE composite dropped to 79.2 kJ/m^2 , and that of the 9% PTFE composite further dropped to 76.6 kJ/m^2 , but all remained above 75 kJ/m^2 . The

decrease in impact strength is mainly attributed to the inherent brittleness of PTFE itself and the weak interfacial adhesion caused by its low surface energy; during stress, it easily debonds from the matrix forming crack sources. With increasing PTFE content, agglomeration intensifies and interfacial defects increase, further affecting the toughness of the composite [21-22].

3.6 Hydrophobic Properties of Composites

Figure 9 shows the water contact angle and water absorption rate test results of the composites. Figure 9(a) indicates that the contact angle of the composite without PTFE was 70.4°, exhibiting hydrophilicity. With increasing PTFE content, the contact angle of the composite gradually increased; when PTFE was 5%, the contact angle reached 86.5°, indicating enhanced surface hydrophobicity [23]. This is because fluorine atoms in the PTFE molecule cover the entire molecular chain surface, forming a low surface energy structure (surface energy ≈ 18 mN/m); according to Young's equation, an increase in contact angle indicates a decrease in material surface energy [24].

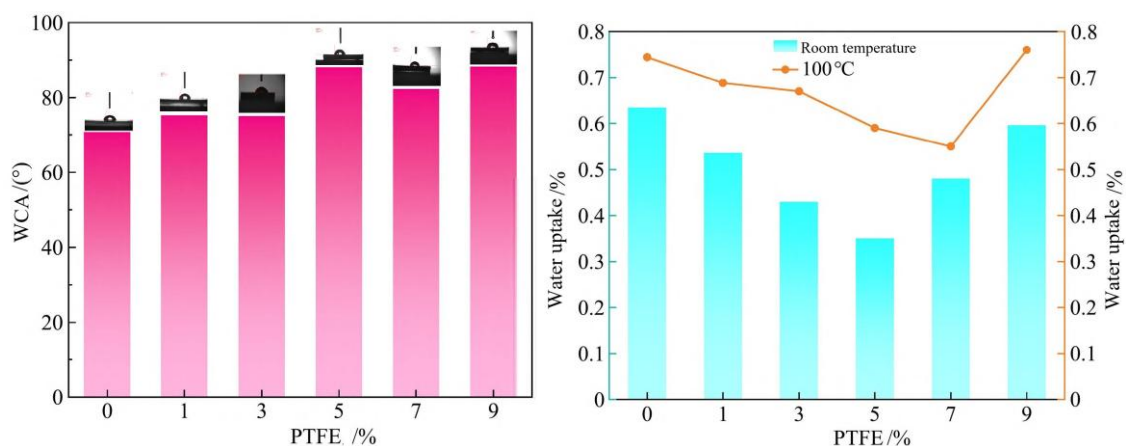


Figure 9 Hydrophobic properties of composites

Figure 9(b) shows that the water absorption rate of composites under ambient and high-temperature conditions exhibited a trend of decreasing first and then increasing. When the PTFE mass fraction was 5%, the composite had the lowest ambient water absorption rate of 0.35%; while the high-temperature water absorption rate was lowest at 0.5% when PTFE was 7%. The strong hydrophobicity of the F element in PTFE and its protective effect on the carbon chain effectively prevent water molecule penetration, and PTFE filling pores reduces the overall porosity of the material. However, when PTFE content is too high, due to differences in surface polarity between PTFE, resin, and glass fiber cloth, unavoidable micro-pores form at the interface. With increasing PTFE content, the number of interfacial micro-pores increases, causing water absorption rate to rebound. Nevertheless, all sample water absorption rates were below 1%, meeting electronic application requirements (IPC-4101 requires <1.5%).

This work presents a targeted material design that addresses the long-standing trade-off between dielectric performance and thermal reliability in high-frequency PCB substrates. By filling the pores of silane-modified glass fiber cloth with polytetrafluoroethylene (PTFE) and using bismaleimide-triazine (BT) resin as the matrix, the composite achieves a balanced property profile aligned with 5G/6G mid-to-high frequency demands. At an optimal 5 wt% PTFE loading, the material delivers a dielectric constant of 3.4 and dielectric loss of 0.003 at 10 GHz, representing reductions of $\sim 8\%$ and $\sim 50\%$ compared to the pure BT system, while maintaining a high glass transition temperature of 250°C and excellent thermal stability (800°C char yield: 76.63%). Mechanistically, these improvements arise from the synergistic interplay of three factors: (1) the ultra-low polarizability of PTFE's C-F bonds suppresses electronic and orientation polarization; (2) pore-filling minimizes air-resin interfacial polarization losses; and (3) enhanced interfacial bonding via KH570 restricts molecular chain mobility. Compared to commercial alternatives, this system offers a compelling middle ground—its dielectric performance approaches that of hydrocarbon resins while retaining BT's superior processability and heat resistance, positioning it as a cost-effective candidate for millimeter-wave antennas and RF front-end modules where

extreme low-loss materials like LCP or pure PTFE would be economically or technically prohibitive.

Despite these advances, the study also reveals critical limitations tied to PTFE's intrinsic properties. The most prominent challenge is the ~40% increase in Z-axis CTE (to $45 \times 10^{-6} \text{ }^\circ\text{C}^{-1}$ at 5 wt% PTFE), driven by PTFE's inherently high thermal expansion and interfacial stress accumulation. Although this value meets the IPC-4101 threshold ($<60 \times 10^{-6} \text{ }^\circ\text{C}^{-1}$), it still poses risks for multilayer PCB reliability, particularly in high-layer-count designs subject to repeated thermal cycling. Excess PTFE (>5 wt%) further exacerbates interfacial defects, leading to agglomeration, reduced flexural strength (~11% drop at 9 wt%), and slight dielectric loss rebound. Additionally, the reliance on a single silane coupling agent (KH570) suggests potential for further optimization through hybrid sizing agents or nano-filler incorporation to mitigate CTE without compromising dielectric gains. Future work should focus on multi-scale interface engineering—such as gradient PTFE distribution or low-CTE inorganic fillers—to decouple the conflicting relationships between dielectric, thermal, and dimensional stability. From an application standpoint, the material's residual moisture resistance (water absorption <0.5%) and robust mechanical retention (>570 MPa flexural strength) support its viability in real-world deployment, though long-term aging tests under combined thermal-humidity-electrical stress remain necessary to validate lifecycle reliability. Overall, this study provides a pragmatic pathway for developing next-generation PCB substrates that balance performance, manufacturability, and cost for evolving high-frequency communication infrastructure.

4. Conclusion

(1) Surface modification of glass fiber cloth using the KH570 silane coupling agent successfully grafted Si–O–Si covalent bonds and organic functional groups onto its surface, significantly improving the interfacial bonding strength between glass fibers, PTFE, and the BT resin matrix.

(2) When the PTFE mass fraction was 5%, the prepared PTFE/BT/GF composite achieved optimal comprehensive performance: dielectric constant and dielectric loss were 4.3 and 0.006 at 1 MHz, and 3.4 and 0.003 at 10 GHz, respectively; the glass transition temperature reached 250°C, an increase of 25°C compared to the pure BT system; the char yield at 800°C reached 76.63%, an increase of about 17.55%; flexural strength remained at 574.7 MPa, and the water contact angle increased to 86.5°.

(3) Dielectric property analysis indicates that the introduction of PTFE significantly improved the high-frequency dielectric properties of the composite by reducing the polarization degree, filling pores to decrease interfacial polarization loss, and restricting the orientation movement of polar groups. The three relaxation peaks at 1 MHz correspond to interfacial polarization, dipolar orientation polarization, and side-chain relaxation, respectively; the addition of PTFE caused peak shifts; the dipolar relaxation peak of BT resin in the 10 GHz band gradually disappeared with increasing PTFE addition.

(4) The introduction of PTFE improved the thermal stability and hydrophobicity of the material, but due to its own high coefficient of thermal expansion ($100\text{--}130 \times 10^{-6} \text{ }^\circ\text{C}^{-1}$) and interfacial CTE mismatch, the Z-axis CTE of the composite increased (approximately $45 \times 10^{-6} \text{ }^\circ\text{C}^{-1}$ at 5% PTFE); although this meets the IPC-4101 standard ($<60 \times 10^{-6} \text{ }^\circ\text{C}^{-1}$), further optimization is still required.

References

- [1] LI Huilu, XIA Ting, SU Jianfeng, et al. Research progress of carbon-hydrogen resin high-frequency copper clad laminate[J]. *Insulating Materials*, 2024, 57(1): 1-8.
- [2] SHI Jianying. How to solve the application of epoxy resin in high-performance copper-clad laminates[C]//*Proceedings of the 2024 China Copper Foil Board Industry High-level Forum*, 2024.
- [3] ZHU Xiaomeng. Preparation and performance study of bicomponent polyimide/cyanate ester hybrid resin system[D]. Harbin: Heilongjiang Academy of Sciences-Petroleum Chemistry Research Institute, 2020.
- [4] QIAO Yajing. Research on the co-curing of epoxy resin/cyanate ester resin and the preparation of composite materials[D]. Beijing: Beijing University of Chemical Technology, 2025.
- [5] AS A, MARNOT C E A, FALLON J J, et al. Material extrusion-based additive manufacturing with blends of

- polypropylene and hydrocarbon resins[J]. ACS Applied Polymer Materials, 2019, 2(2): 911-921.
- [6] WANG Xu, WANG Qi, HOU Hongbo, et al. Preparation and properties of glass fiber reinforced BT resin composites[J]. Plastics Technology, 2022, 50(9): 6-9.
- [7] WANG Qi. Synthesis, modification and composite material research of bismaleimide resin[D]. Zigong: Sichuan University of Science and Engineering, 2022.
- [8] ZHANG Lin, LI Yuhai. The properties and application status of polytetrafluoroethylene[J]. Innovation and Technology Herald, 2012(4): 111-112.
- [9] FANG Hongqiang. Preparation and performance study of ptfe/glass fiber composite materials[D]. Xi'an: Journal of Northwestern Polytechnical University, 2018.
- [10] HU Xingyu. Study on the curing mechanism and properties of low dielectric MOFs/bis-maleimide-triazine resin nanocomposites[D]. Chongqing: Chongqing Technology and Business University, 2021.
- [11] XIE Tianhua, WANG Can, JIANG Jianchao, et al. Modification of flame-retardant bismaleimide-triazine resin and its glass fiber cloth copper clad laminate[J]. Journal of Composite Materials, 2026, 43(3): 1441-1449.
- [12] SUN M, HUANG J, NING X. High silica fiberglass cloth/PTFE composites: interfacial bonding and dielectric property enhancement[J]. Polymer Composites, 2024, 45(18): 16945-16954.
- [13] MUKHTAR M, KLOSTERMAN D, MORGAN A B. Preparation, cure, characterization, and mechanical properties of reactive flame-retardant cyanate ester/epoxy resin blends and their carbon fiber reinforced composites[J]. Composites Part B: Engineering, 2024, 282: 16.
- [14] WENG X, SONG Y, XIONG Z, et al. Preparation of micro-nano PBO fiber/polytetrafluoroethylene composite papers with excellent dielectric properties for high frequency wave-transparent applications[J]. Composites Part A: Applied Science and Manufacturing, 2025, 198: 109078.
- [15] ZHOU D, WANG Y, REN Y. Coupling agent modified MGSA ceramic powder filled PTFE composite materials: High thermal conductivity and low dielectric loss of substrate materials for microwave high frequency and high-speed communication[J]. Journal of Alloys and Compounds, 2025: 1012.
- [16] DU Liqiang, HE Jianyun, DAI Haiyang, et al. The influence of in-situ fibrillated PTFE on the electromagnetic shielding performance of PP/CNT micro-hole injection-molded foaming materials[J]. Plastics, 2024, 53(1): 28-31.
- [17] DHANUMALAYAN E, JOSHI M G. Performance properties and applications of polytetrafluoroethylene(PTFE)-a review[J]. Advanced Composites and Hybrid Materials, 2018, 1(2): 247-268.
- [18] YU Y, CHEN X, HOU D, et al. Fluorinated polydopamine shell decorated fillers in polytetrafluoroethylene composite for achieving highly reduced coefficient of thermal expansion[J]. Polymers, 2024, 16(7): 20734360.
- [19] YAN Xiangyu, YUAN Ying, ZHANG Shuren, et al. Preparation of SiO₂-TiO₂/polytetrafluoroethylene composite materials and their thermal expansion properties[J]. Journal of Composite Materials, 2013, 30(6): 108-113.
- [20] WANG Xiaoyan, SUN Bo. Preparation and Properties of Polytetrafluoroethylene-Calcium Carbonate Super hydrophobic Composite Coating[J]. Synthetic resins and plastics, 2019, 36(4): 23-25, 37.
- [21] YANG Fan, YAN Hongxia, LI Pengbo, et al. PTFE/F-CNTs/BMI Research on Ternary Composite Friction Materials[J]. Mechanical Science and Technology, 2012, 31(1): 159-162.
- [22] ZHANG QiuJun, YANG Liu, SHU Can, et al. Preparation and properties of polytetrafluoroethylene/epoxy resin composite coatings[J]. Electroplating and Coating, 2025, 44(4): 127-135.
- [23] LI Xiaodong, ZHANG Qinghong, YE Jinlin. Some theoretical issues in climatological research[J]. Journal of Peking University: Natural Science Edition, 1999, 35(1): 101-106.
- [24] ZHONG Wenfa. Application of nonlinear programming in combustible material allocation[C]//ZHAO Wei. Theory and Application of Operations Research: Proceedings of the Fifth Congress of the China Operational Research Society. Xi'an: Xidian University Press, 1996: 468-471.